JCTC Journal of Chemical Theory and Computation

Peptide Partitioning and Folding into Lipid Bilayers

Jakob P. Ulmschneider,*,† Jacques P. F. Doux,‡ J. Antoinette Killian,‡ Jeremy C. Smith,§ and Martin B. Ulmschneider*,‡

IWR, University of Heidelberg, Germany, Department of Chemistry, University of Utrecht, Utrecht, The Netherlands, and Oak Ridge National Laboratory, Oak Ridge, Tennessee

Received May 20, 2009

Abstract: The folding and partitioning of WALP peptides into lipid bilayers is characterized using atomic detail molecular dynamics simulations on microsecond time scales. Elevated temperatures are used to increase sampling, and their suitability is validated via circular dichroism experiments. A new united atom parametrization of lipids is employed, adjusted for consistency with the OPLS all-atom force field. In all simulations secondary structure forms rapidly, culminating in the formation of the native trans-membrane helix, which is demonstrated to have the lowest free energy. Partitioning simulations show that peptide insertion into the bilayer is preceded by interfacial folding. These results are in excellent agreement with partitioning theory. In contrast, previous simulations observed unfolded insertion pathways and incorrectly report stable extended configurations inside the membrane. This highlights the importance of accurately tuning and experimentally verifying force field parameters against microsecond time scale phenomena.

How helical peptides fold and integrate into lipid bilayer membranes remains one of the most intriguing processes in biophysics. Unfortunately, these folding pathways cannot currently be directly spatially and temporally resolved in experiments. In principle, computer simulations can provide the required information, as they can now reach >μs time scales. However, simulation accuracy requires careful calibration and verification of force field parameters. We have recently reported a new set of OPLS-UA lipid parameters tuned against a large set of experimental data.[1] Here we present the application of these parameters in ab initio simulations of peptide bilayer folding and insertion simulations. The results demonstrate the importance of accurate parameters in obtaining the correct partitioning pathway.

Partitioning theory,[2] and previous simulations using implicit membrane models,[3,4] strongly suggest a folded insertion pathway for hydrophobic peptides and a stable trans-membrane helix as the native state: the high cost of desolvating exposed peptide bonds (estimated at ~4 kcal/mol/bond)[5] dictates that the transfer of solvated peptides into a hydrocarbon phase should follow a two-stage pathway, where helical segments fold at the phase boundary prior to insertion (see Figure 1A).[6,7] A recent microsecond molecular dynamics simulation[8] directly examined the folding and partitioning of synthetic WALP peptides[9] into explicit lipid bilayer membranes. However, this study reported both an unfolded insertion pathway as well as a nonhelical native state in the bilayer. The disagreement of this result with theory may arise from either errors in the GROMOS96(43a2)/Berger (G96/Berger) parameters, or it might be a consequence of the elevated temperature of 80 °C used in the simulations to enhance sampling.

Since no experimental data are available for WALP at elevated temperatures we have measured the peptide secondary structure as a function of temperature using circular dichroism spectroscopy. These experiments show that the helicity of WALP in DMPC lipid vesicles decreases by less than 4% when the temperature is increased from 25° to 90 °C (see Figure 2, for experimental details see the Supporting Information). Equivalent folding simulations can therefore also be performed at elevated temperatures, as the native state is highly thermostable. This has the advantage of greatly speeding up conformational sampling. The destabilization of the native state helix in ref 8 therefore strongly points toward a problem with either the protein force field or the 'Berger' lipid parameters.[10] To address this problem, we have recently developed a new set of united-atom lipid parameters for use in combination with the OPLS all-atom (OPLS-AA) force field for the peptide.[1] For this, the 'Berger' lipid parameters were modified to permit a nonbonded scale factor of 0.5 for 1−4 interactions, which is the standard for OPLS-AA.[11] In addition, the hydrocarbon Lennard-Jones parameters of the lipid tails were changed, as the strength of the interactions in the original set was too weak. These new lipid parameters were used to study the folding and partitioning of WALP, resulting in markedly different behavior to the previous simulations (Methods are given in the Supporting Information).

* Corresponding author e-mail: jakob@ulmschneider.com (J.P.U.), martin@ulmschneider.com(M.B.U.).

† University of Heidelberg.

‡ University of Utrecht.

§ Oak Ridge National Laboratory.

10.1021/ct900256k CCC: $40.75
Published on Web 07/23/2009

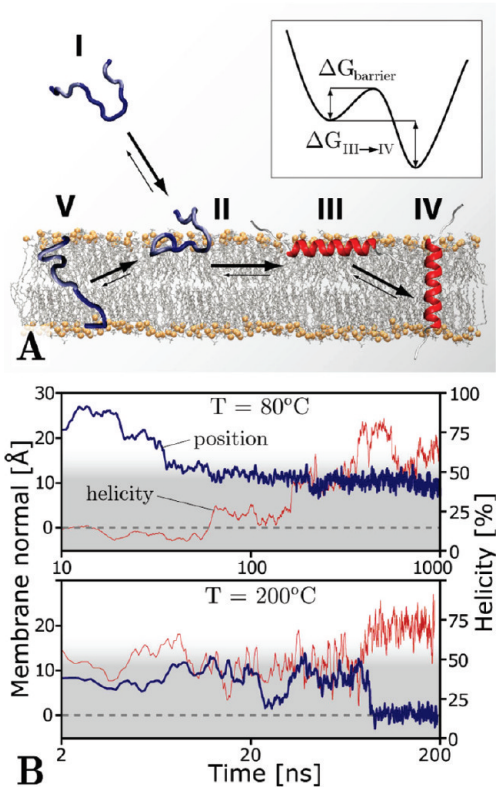

Figure 1. **A:** Schematic of peptide partitioning into lipid bilayer membranes. Hydrophobic peptides are generally unfolded in solution (I). Membrane insertion occurs after interfacial adsorption (II). Two partitioning pathways have been proposed: Unfolded (I→II→V→IV) and folded insertion (I→II→III→IV). Energetic arguments strongly favor a folded partitioning pathway. **B:** Adsorption, folding and partitioning of WALP16 in a DPPC bilayer. The helicity (red) and position along the membrane normal (blue) show peptide absorption and interfacial folding at 80 °C (**upper panel**), followed by folded insertion after ~80 ns at an elevated temperature of 200 °C (**lower panel**).

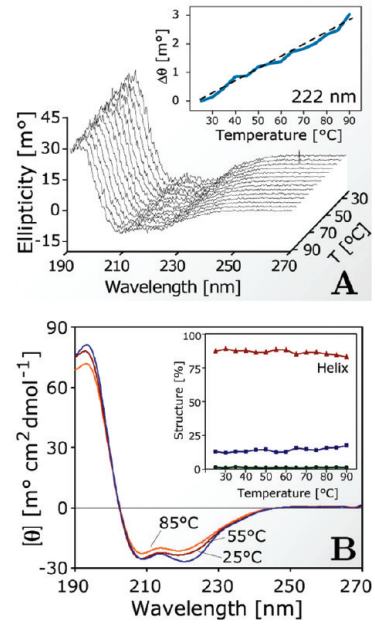

Figure 2. Circular dichroism measurements of the secondary structure of WALP16 in DMPC vesicles over a temperature range of 25−90 °C (for details see the Supporting Information). **A:** The spectra show three distinctive extrema at 208, 222 nm, and 193 nm, which are characteristic of alpha-helices embedded in the lipid bilayer membrane of vesicles. The 222 nm line (inset) shows linear behavior, demonstrating that no melting takes place over the full temperature range. **B:** The position of the peaks in the smoothed spectra show no significant lateral shifts. Secondary structure analysis (inset) shows that the peptide remains helical over the entire temperature range with a loss of helicity of less than 4%. Similar results were obtained in DPPC (manuscript in preparation).

In the simulations two types of bilayer-forming lipid (DPPC, DMPC) were used, and the peptide lengths (WALP16, WALP23) were varied. In addition to the force field changes reported, folding was also studied at lower temperatures (50 °C), where sampling still turned out to be rapid enough to capture folding events within the 1 μs time frame of the simulations.

Two sets of starting configurations were generated, with extended WALP peptides inserted into bilayers in a membrane spanning configuration, and outside the membrane in the solvent. The folding results of the different systems starting with the extended peptide embedded in the membrane (WALP16 in DMPC at 50 °C, WALP16 in DPPC at 80 °C, and WALP23 in DPPC at 80 °C) are summarized in Figure 3. All peptides rapidly form secondary structure, culminating in stable membrane spanning helices within 1 μs.

The helices correspond to the experimentally observed native state. The initial phase of all simulations is characterized by a rapid collapse of the peptide from its extended conformation. Within 50−100 ns, the water-exposed parts of the peptides are buried in the bilayer, and the enthalpy drops by ~10 kcal/mol per residue in all simulations. The collapse is concomitant with a buildup of helical turns (see Figure 4B). The significantly slower sampling rate of WALP16 in DMPC at 50 °C results in the peptide remaining unfolded but fully inserted from 170 to 260 ns, thus enabling energetic separation of the burial from the folding process. The result is an enthalpic stabilization of the native helix over the unfolded inserted conformations of ~2.6 ± 1.8 kcal/mol per residue. This is of the same order of magnitude as the ~4 kcal/mol estimated previously[5,12] and somewhat smaller than the 5−10 kcal/mol reported by Nymeyer et al.[13] Thus, the helix is enthalpically strongly favored over competing structures, in agreement with experimental evidence and in contrast to the results obtained with different force fields.[8]

To assess the thermodynamic stability of the peptides, we obtained the free energy as a function of helicity by plotting the logarithm of a population histogram over the final 500 ns (see Figure 4A, details in the Supporting Information). For the OPLS-AA protein in combination with the newly parametrized lipids unfolded insertion is highly unfavorable, even at high temperatures of 80 °C, and no unfolding is observed on the microsecond time scale of the simulations, indicating the transmembrane helix is the global free energy minimum. These results are independent of the lipid used, with indistinguishable folding patterns for WALP16 embedded into DMPC and DPPC bilayers. Increasing the hydrophobic core length of WALP from 16 to 23 residues showed no marked effect on the folding process, and except for a slight increase in the tilt angle of the native state from 18° ± 5° to 30 ± 9° no difference is

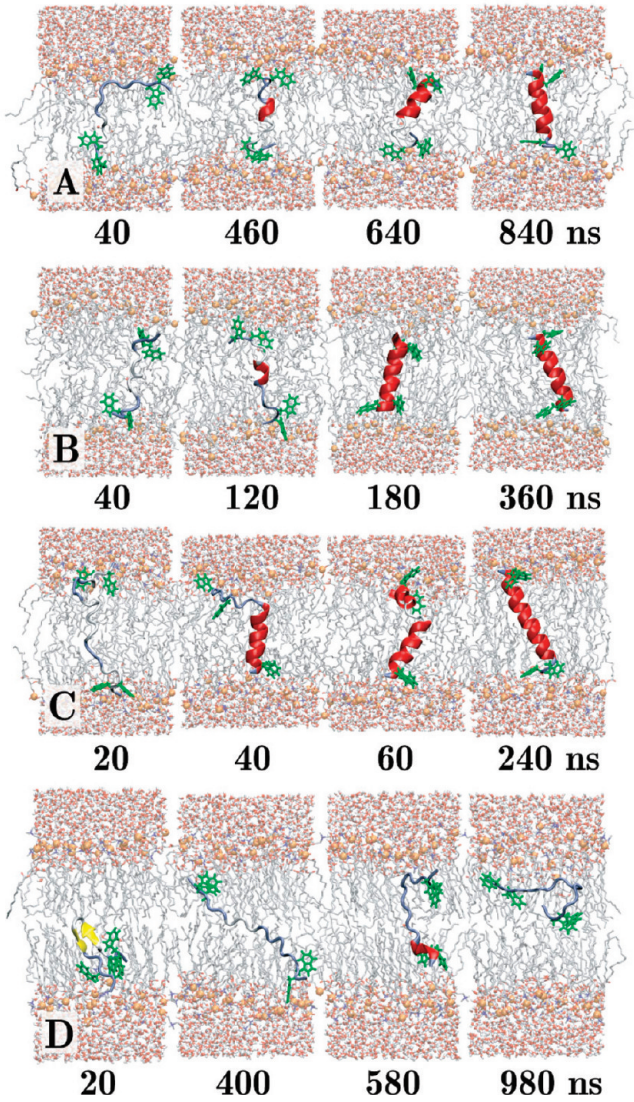

Figure 3. Intramembrane folding of WALP in explicit lipid bilayer membranes with the OPLS-AA force field and newly derived lipid parameters: **A:** WALP16 in DMPC at 50 °C. **B:** WALP16 in DPPC at 80 °C. **C:** WALP23 in DPPC at 80 °C. **D:** WALP16 in DPPC at 50 °C using the G96/Berger force field and the SPC water model. A large number of unfolded and beta-structures are sampled.

discernible. The tilt angle increase is consistent with experimental observations[14] and with results from implicit membrane models.[4,15,16] In addition, no major dependence of the equilibrium properties on the temperature is visible. The folding kinetics of WALP16 at 50 °C is markedly slower with 600 ns required to reach >50% helicity, compared to 140 ns at 80 °C. The folding pathway, however, remains similar.

The present results contrast sharply with previous WALP16 simulations in DMPC and DPPC bilayers.[8] In ref 8 unfolded conformations, stably inserted into the bilayer, dominate at 80 °C, with the peptide oscillating between deeply inserted completely extended and misfolded conformations. The transient formation of a membrane spanning helix after ~1.9 μs did not lead to further energetic stabilization, and the helix remained stable for only ~200 ns before unfolding again.[8] Furthermore, a control simulation starting from an inserted helix was found to unfold after ~300 ns, indicating that it is not stable at 80 °C.

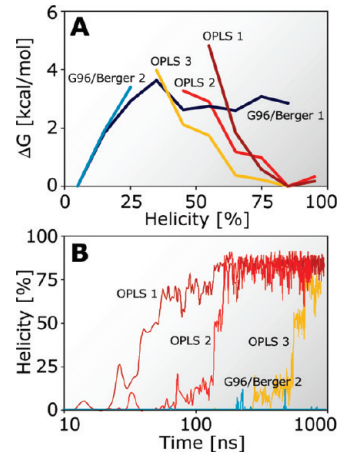

Figure 4. **A:** Free energies as a function of peptide helicity. All OPLS simulations correctly identify the native helical state as the free energy minimum. The G96/Berger systems show unfolded free energy minima. **B:** Helicity against simulation time for the OPLS systems (OPLS 1 = WALP16 in DPPC at 80 °C; OPLS 2 = WALP23 in DPPC at 80 °C; OPLS 3 = WALP16 in DMPC at 50 °C; G96/Berger 1 = WALP16 in DPPC at 80 °C; G96/Berger 2 = WALP16 in DPPC at 50 °C). For the G96/Berger simulations helices form only sporadically and unfold again rapidly.

The comparatively long time scales required to unfold the peptide suggests the state is kinetically trapped, with a thermally accessible barrier to unfolding/refolding. Simulations at 50 °C give similar results, with the peptide remaining inserted in an unfolded configuration (Figure 3D). However, the lack of folding events in this simulation, and the nonreversibility of the folding in all the OPLS simulations indicate that despite the microsecond scale the free energy profiles in Figure 4 should be considered only as rough estimates.

To investigate whether some of the observed differences can be explained by a helical bias in the underlying protein force field, control simulations (500 ns each) of WALP16 starting from an α-helical conformation were performed in water boxes (~2000 water molecules) at 27 and 80 °C, with both the G96 and OPLS-AA force field. As expected for a completely hydrophobic peptide, WALP16 quickly unfolds in all simulations, exposing the polar backbone to the water. The average helicity is ~10% over the final 100 ns in all four simulations. Thus, the difference in stability seen in the partitioning simulations is not due to an intrinsic preference of the OPLS-AA parameters favoring the helical state.

Spontaneous folding and insertion of WALP16 was also studied starting from unstructured conformations placed in bulk solvent. Hydrophobic peptides are thought to follow the 'folded insertion' pathway[6] illustrated in Figure 1A, where the unstructured peptide (I) is first adsorbed to the interface (II), which catalyzes folding (III), finally allowing the peptide to insert (IV). Hydrogen bond formation greatly decreases the cost of partitioning peptide bonds, favoring folded structures in the membrane. This model is supported by our simulations: WALP16 at 80 °C is adsorbed to the surface after ~25 ns, where it forms an interfacial helix after ~400 ns (see Figure 5A, the corresponding helicity and z-position is given in Figure 1B). The helix remains stable, sandwiched between the hydrophobic core and the polar lipid head groups. However, insertion is not

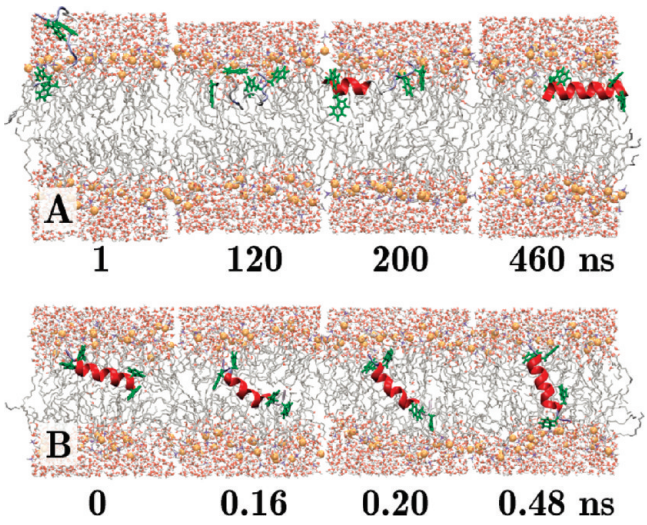

Figure 5. **A:** Adsorption and interfacial folding of WALP16 at 80 °C. **B:** Insertion at 200 °C after 80 ns. The insertion event is rapid taking less than 0.5 ns to complete.

observed within the microsecond time frame of the simulation, indicating the presence of a kinetic barrier to partitioning, due to the need to translocate two bulky TRP residues across the hydrophobic core of the bilayer from one interface to the other, their preferred position along the membrane normal. To probe the thermal surmountability of the barrier, the simulation temperature was increased to 200 °C. Figure 1B shows that WALP remains predominantly helical at this temperature, and the barrier is crossed after ~80 ns. At 80 °C, the transmembrane state of WALP16 is strongly stabilized compared to the interfacial helix by $\Delta H_{\mathrm{III}\rightarrow\mathrm{IV}} = -12 \pm 4.8$ kcal/mol or -0.8 ± 0.3 kcal/mol per residue. From the thermal accessibility of the kinetic barrier at 200 °C we estimate its height to be roughly ~20 kcal/mol.

The present results are very different from the interfacial folding simulations in refs 8 and 13, which observed neither an interfacial helical state nor a barrier to insertion, with WALP favoring the unfolded inserted (V) state. In contrast, the present OPLS simulations show that WALP16 follows the pathway illustrated in Figure 1A. The interfacial insertion barrier is probably not a general feature for all hydrophobic peptides and could vanish if bulky headgroup anchoring side chains are replaced by e.g., alanines or leucines. In this case the surface adsorbed folded state will only be populated during a short transition time, and the whole process might show concomitant folding and insertion. However, unfolded insertion will be unfavorable irrespective of the particular hydrophobic sequence.

The partitioning behavior illustrated in Figure 5 matches previous results on WALP peptides obtained with generalized Born implicit membrane models. These implicit membrane simulations also predicted an interfacial folding path to the final transmembrane helix and at a fraction of the computational cost.[3,4,17] However, implicit models are generally limited by a poor representation of structural features such as the complex lipid headgroup environment and entropic effects due to lipid tail order. Our results demonstrate that ab initio peptide partitioning studies can now also be performed in fully explicit lipid bilayers. This greatly increases both the accuracy and scope of membrane protein simulations. Explicit models also allow for studies of peptide induced bilayer deformations via hydrophobic mismatch, pore formation events, and membrane fusion or lysis. In addition, the lipid composition of the bilayer can be varied easily. Explicit treatment also directly accounts for structural water molecules, which often form part of an intricate system of hydrogen bonds that interconnect helices and protein subunits. Reorganization of these highly dynamic hydrogen bonding networks is one of the key drivers of conformational changes and associated function.

However, great care must be taken to ensure that the protein and lipid force fields are well balanced. In the future, this can be best achieved by comparing experimental peptide partitioning results with direct microsecond time scale folding simulations and thus obtaining improved force field parameters that reproduce partitioning data of whole peptides. The resulting models open the possibility to provide accurate atomic detail insights into complex biophysical membrane processes, such as antimicrobial peptide-induced membrane lysis or spontaneous assembly of membrane proteins from fragments.

Acknowledgment. This research was supported by the Human Frontier Science Program (M.B.U.) and BIOMS (J.P.U.). J.C.S. was supported by a DOE Laboratory Directed Research and Development award.

Supporting Information Available: Methods. This material is available free of charge via the Internet at http://pubs.acs.org.

References

(1) Ulmschneider, J. P.; Ulmschneider, M. B. *J. Chem. Theory Comput.* 2009. in press (available online).

(2) White, S. H.; Wimley, W. C. *Annu. Rev. Biophys. Biomol. Struct.* **1999**, *28*, 319.

(3) Im, W.; Brooks, C. L. *Proc. Natl. Acad. Sci. U.S.A.* **2005**, *102* (19), 6771.

(4) Ulmschneider, M. B.; Ulmschneider, J. P. *Mol. Membr. Biol.* **2008**, *25* (3), 245.

(5) White, S. H. *Adv. Protein Chem.* **2006**, *72*, 157.

(6) Jacobs, R. E.; White, S. H. *Biochemistry* **1989**, *28* (8), 3421.

(7) Popot, J. L.; Engelman, D. M. *Biochemistry* **1990**, *29* (17), 4031.

(8) Ulmschneider, M. B.; Ulmschneider, J. P. *J. Chem. Theory. Comput.* **2008**, *4* (11), 1807.

(9) Killian, J. A. *FEBS Lett.* **2003**, *555* (1), 134.

(10) Berger, O.; Edholm, O.; Jahnig, F. *Biophys. J.* **1997**, *72*, 2002.

(11) Jorgensen, W. L.; Maxwell, D. S.; Tirado-Rives, J. *J. Am. Chem. Soc.* **1996**, *118* (45), 11225.

(12) BenTal, N.; Sitkoff, D.; Topol, I. A.; Yang, A. S.; Burt, S. K.; Honig, B. *J. Phys. Chem. B* **1997**, *101* (3), 450.

(13) Nymeyer, H.; Woolf, T. B.; Garcia, A. E. *Proteins* **2005**, *59* (4), 783.

(14) Ozdirekcan, S.; Etchebest, C.; Killian, J. A.; Fuchs, P. F. *J. Am. Chem. Soc.* **2007**, *129* (49), 15174.

(15) Ulmschneider, J. P.; Ulmschneider, M. B.; Di Nola, A. *Proteins* **2007**, *69*, 297.

(16) Sengupta, D.; Meinhold, L.; Langosch, D.; Ullmann, G. M.; Smith, J. C. *Proteins* **2005**, *58* (4), 913.

(17) Ulmschneider, J. P.; Ulmschneider, M. B. *Proteins* **2009**, *75* (3), 586.

CT900256K